Mon. Not. R. Astron. Soc. **000**, 000–000 (0000) Printed 25 July 2017 (MN LATEX style file v2.2)

SDSS-IV MaNGA: Slow Rotators Quench Faster than Fast Rotators

R. J. Smethurst,[1] M. Merrifield,[1] K. L. Masters,[2] C. J. Lintott,[3] A.-M. Weijmans,[4] A. Aragón-Salamanca,[1], B. Nichol,[2] N. Drory,[5], D. R. Law,[6] J. Brownstein,[7] K. Bundy [8]

[1] *School of Physics and Astronomy, The University of Nottingham, University Park, Nottingham, NG7 2RD, UK*
[2] *Institute of Cosmology and Gravitation, University of Portsmouth, Dennis Sciama Building, Barnaby Road, Portsmouth, PO13FX, UK*
[3] *Oxford Astrophysics, Department of Physics, University of Oxford, Denys Wilkinson Building, Keble Road, Oxford, OX13RH, UK*
[4] *School of Physics and Astrononomy, University of St Andrews, North Haugh, St Andrews, Fife, KY169RJ, UK*
[5] *McDonald Observatory, The University of Texas at Austin, 1 University Station, Austin, TX 78712, USA*
[6] *Space Telescope Science Institute, 3700 San Martin Drive, Baltimore, MD 21218, USA*
[7] *Department of Physics and Astronomy, University of Utah, 115 S. 1400 E., Salt Lake City, UT 84112, USA*
[8] *University of California, Santa Cruz, 1156 High St. Santa Cruz, CA 95064, USA*

25 July 2017

ABSTRACT

We present a study of the star formation histories of fast and slow rotators. Using data from the MaNGA IFU survey, we identify a sample of non-regular rotators undergoing quenching, to which we stellar mass match a sample of quenching regular rotators, resulting in a total of 314 galaxies. We use $u-r$ and $NUV-u$ colours from SDSS and GALEX and an existing inference package, STARPY to conduct a first look at the onset time and exponentially declining rate that quenching has occurred in these galaxies. We find that the distribution of quenching rates across the two populations is significantly (2.9σ) different, suggesting that fast and slow rotators have different evolutionary histories despite similar current star formation rates. We find that quenching is more likely to occur at a rapid rate ($\tau \lesssim 1$ Gyr) for slow rotators than for fast rotators, in agreement with theories suggesting slow rotators are formed in dry major mergers. We discuss how the total gas mass of a merger, rather than the merger mass ratio, may decide a galaxy's ultimate kinematic fate.

Key words: galaxies – photometry, galaxies – statistics, galaxies – morphology

1 INTRODUCTION

Recent work studying the early-type galaxy population has revealed that it is actually composed of two separate populations. The majority of early-types are rotationally supported (Emsellem et al. 2011) with ~ 7 times the number of galaxies with kinematic discs ('fast' rotators), than those with either dispersion dominated kinematics ('slow' rotators) or kinematically decoupled cores (Cappellari et al. 2007; Emsellem et al. 2007, collectively referred to as 'non-regular' rotators). This has led to the proposal of a revision of Hubble's morphological classification scheme in the form of a 'comb' (Cappellari 2016), whereby the evolution of a galaxy, from disc to bulge-dominated, takes place along a 'tine' of the comb as a fast rotator, always retaining an underlying disc. If the discs of these regular rotators are destroyed, they then evolve along the 'handle' of the comb to become slow rotators.

Dry major mergers are considered the most likely process to produce slow rotators (Duc et al. 2011; Naab et al. 2014) as they can rapidly destroy the disc dominated nature of a galaxy (Toomre & Toomre 1972). Fast rotators, are thought to evolve from the slow build up of a galaxy's bulge over time, eventually overwhelming the disc. This growth is thought to occur via gas-rich major or minor mergers (Duc et al. 2011) and by gas accretion (Cappellari et al. 2013; Johnston et al. 2014) which can produce a bulge dominated but rotationally supported galaxy (which would be visually classified as an early-type in the Hubble classification scheme).

Both major mergers and minor mergers have been postulated as quenching mechanisms (Hopkins et al. 2008; Snyder et al. 2011; Hayward et al. 2014), with major mergers thought to cause a much faster quench of the remnant galaxy than a minor merger (Lotz et al. 2008, 2011). Gas accretion is also thought to cause quenching due to the large gravitational potential of the bulge which builds as the accreted gas sinks to the centre of the galaxy. This prevents the disc from collapsing and forming stars in a process which is referred to as morphological quenching (Fang et al. 2013). If fast and slow rotators form via these different mechanisms, we should therefore also expect to find a difference in the star formation histories of quenching or quenched fast and slow rotators.

This is a first look at this problem using an existing Bayesian star formation inference package, STARPY, to determine the quenching histories of a sample of fast and slow rotators. We use broadband optical, $u-r$ and near-ultraviolet $NUV-u$ colours from SDSS and GALEX to infer both the time and rate that quenching has occurred in each galaxy. We aim to determine whether rotationally supported and dispersion dominated galaxies have different quenching histories.

The zero points of all magnitudes are in the AB system. We adopt the WMAP Seven-Year Cosmology (Jarosik et al. 2011) with $(\Omega_m,\ \Omega_\Lambda,\ h) = (0.26, 0.73, 0.71)$.

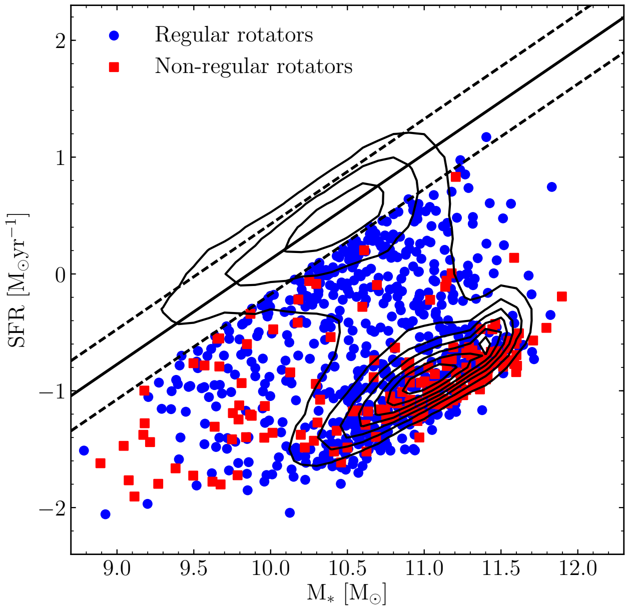

Figure 1. Stellar mass against star formation rate for the Q-MANGA-GALEX sample with regular (blue circles) and non-regular (red squares) rotators identified. Shown also are the contours for the entire MPA-JHU sample (black contours; i.e. SDSS DR7). The solid line shows the SFS as defined by Peng et al. (2010) at the average redshift of the Q-MANGA-GALEX sample with $\pm 1\sigma$ shown by the dashed lines. Note that the galaxies in the Q-MANGA-GALEX sample are chosen to be more than 1σ below the SFS as defined at their observed redshift and stellar mass (see Section 2.3).

2 DATA AND METHODS

2.1 SDSS & GALEX Photometry

We use optical photometry from the Sloan Digital Sky Survey Data Release 7 (SDSS; York et al. 2000; Abazajian et al. 2009). We use the Petrosian magnitude, `petroMag`, values for the u (3543Å) and r (6231Å) wavebands provided by the SDSS DR7 pipeline (Stoughton et al. 2002). Further to this, we also required NUV (2267Å) photometry from the GALEX survey (Martin et al. 2005). Observed fluxes are corrected for galactic extinction (Oh et al. 2011) by applying the Cardelli, Clayton, & Mathis (1989) law. We also adopt k-corrections to $z = 0.0$ and obtain absolute magnitudes from the NYU-VAGC (Blanton et al. 2005; Padmanabhan et al. 2008; Blanton & Roweis 2007).

2.2 MaNGA Survey & Data Reduction Pipeline

MaNGA is a multi-object IFU survey conducted with the 2.5 m Sloan Foundation Telescope (Gunn et al. 2006) at Apache Point Observatory (APO) as part of SDSS-IV (Blanton et al. *submitted*). By 2020 MaNGA will have acquired IFU spectroscopy for ~ 10000 galaxies with $M_* > 10^9$ M$_\odot$ and an approximately flat mass selection Wake et al. (2017). The target selection is agnostic to morphology, colour or environment.

In order to obtain spectra, MaNGA makes use of the Baryon Oscillation Spectroscopic Survey (BOSS) spectrograph (Smee et al. 2013). The BOSS spectrograph provides continuous coverage between 3600 $\AA$ and 10300 $\AA$ at a spectral resolution $R \sim 2000$ ($\sigma_{\rm instrument} \sim 77$km s^1).

Complete spectral coverage to $1.5R_e$, a galaxy's effective radius, is obtained for the majority of targets, though a subset have coverage to $2.5R_e$. See Bundy et al. (2015) for an overview of the MaNGA survey. For a further description of the instrumentation used by MaNGA see Drory et al. (2015). For a detailed description of the observing strategy see Law et al. (2015) and for a description of the survey design see Yan et al. (2016).

The raw data was processed by the MaNGA data reduction pipeline (DRP), which is discussed in detail Law et al. (2016). The MaNGA DRP extracts, wavelength calibrates and flux calibrates all fibre spectra obtained in every exposure. The individual fibre spectra are then used to form a regular gridded datacube of $0.5''$ spaxels and spectral channels. The spectra are logarithmically sampled with bin widths of $\log\lambda = 10^{-4}$.

These datacubes are then analysed using the MaNGA data analysis pipeline (DAP); the development of which is ongoing and will be described in detail in Westfall et al. (in preparation). The primary output from the DAP are 2D "maps" (i.e., images) of measured properties, which include flux, stellar-continuum fits, spectral index measurements and absorption- and emission-line properties. The effective radius, R_e, of a galaxy and the ellipticity within it, ϵ_e, are provided for MaNGA galaxies in the NASA Sloan Atlas; we use the values measured with elliptical Petrosian apertures in `v1_0_1` of the catalogue provided in the SDSS Data Release 13 (SDSS Collaboration et al. 2016).

2.3 Data sample

Our galaxy sample is drawn from the 2,777 SDSS galaxies currently observed by the MaNGA survey. We cross-matched these galaxies with a radius of $3''$ to the GALEX survey in order to obtain NUV photometry (see Section 2.1), resulting in 1,413 galaxies.

In this study we wish to investigate the quenching histories of galaxies, therefore we sub-select those galaxies which are below the star forming sequence (SFS). Here we use the global average SFR values quoted in the MPA-JHU catalogue (Kauffmann et al. 2003; Brinchmann et al. 2004, which are corrected for aperture bias). We do not use the MaNGA spectra to calculate SFRs since the bundles only extend to $1.5\ R_e$, which may result in an underestimation of the global SFR of a galaxy.

We select galaxies with a SFR more than 1σ below the SFS of Peng et al. (2010). Since we wish to test whether slow rotators quench at rapid rates, consistent with major mergers, we wish to include those galaxies which have just left the SFS (rather than selection those that are, for example, 3σ below the SFS).

This selection on SFR when applied to the MANGA-GALEX sample results in a sample of 838 quenching or quenched galaxies, which we will refer to as the Q-MANGA-GALEX sample. This sample is shown in Figure 1.

Note that this selection will induce some bias in our sample. Fast rotators are theorised to evolve through processes which provide a fresh supply of gas for star formation, including gas-rich mergers and gas accretion. Therefore this work will only probe a specific subset of the fast rotator population. However, slow rotators are thought to only form through dry major mergers. If this is the case, then a slow rotator can only be formed from a fast rotator within which quenching is already under way. However, simulations have shown that the morphological transformation in a major merger occurs before the SFR drops (e.g. see Sparre & Springel 2016). We should therefore still be able to probe whether this major merger evolution scenario exists in the slow rotator sample.

In order to classify the galaxies in the Q-MANGA-GALEX sample as slow rotators or otherwise, we first calculate the specific stellar angular momentum as defined by Emsellem et al. (2007, 2011);

$$\lambda_{R_e} = \frac{\sum_{i=1}^{N} F_i\ R_i\ |V_i|}{\sum_{i=1}^{N} F_i\ R_i\ (V_i^2 + \sigma_i^2)^{1/2}}, \tag{1}$$

where F_i is the flux in the ith spaxel, R_i the spaxel's distance from the galaxy centre (where $R_i < R_e$, the effective radius of a galaxy), V_i the mean stellar velocity in that spaxel, σ_i the stellar velocity dispersion in that spaxel and N the total number of spaxels. In this work we use the *Python* function provided in the MaNGA DAP to calculate λ_{R_e} using the values of mean flux, radius, stellar velocity and stellar velocity dispersion (corrected for instrumental resolution effects) provided by the MaNGA DAP (see Section 2.2). Velocity dispersion measurements in each spaxel of a galaxy were confirmed to be above the instrument resolution of 77 km s^{-1}.

We then classify galaxies in the Q-MANGA-GALEX sample as regular or non-regular rotators using the definition from Cappellari (2016):

$$\lambda_{R_e} < 0.08 + \frac{\epsilon_e}{4} \qquad \text{with} \qquad \epsilon_e < 0.4. \tag{2}$$

Using this definition reveals 673 (80%) regular rotators and 157 (20%) non-regular rotators in the Q-MANGA-GALEX sample. These galaxies are shown by their velocity maps in Figure 2 along with the definition of a non-regular rotator from Cappellari (2016), shown by the solid black line.

This fraction of non-regular rotators (20%) is slightly higher than that found by previous works (14−17% of early-types in the ATLAS^{3D} sample; Emsellem et al. 2011; Stott et al. 2016). Considering we do not select our sample based upon visual morphology, we would expect a smaller fraction of non-regular rotators than previous works which specifically derived the early-type fraction of non-regular rotators. However, other studies have shown that the non-regular rotator fraction increases with stellar mass Cappellari et al. (2013), up to $\sim 90\%$ at 10^{12} M$_\odot$ Veale et al. (2017). Upon inspection the median stellar mass of the Q-MANGA-GALEX sample is $10^{10.8}$ M$_\odot$, which is higher than the median stellar mass of the ATLAS^{3D} sample at $10^{10.5}$ M$_\odot$.

In order to obtain a sample of slow rotators, one author (RJS) inspected the velocity maps of the 157 non-regular rotators identified in the Q-MANGA-GALEX sample to remove those galaxies which do not possess dispersion dominated kinematics. 56 galaxies exhibiting counter rotation or decoupled rotation were identified, example velocity maps for which are shown in the top row of Figure 3. This resulted in a sample of 101 slow rotators, example velocity maps for which are shown in the middle row of Figure 3.

In order to control for the degeneracies between mass, metallicity and dust we selected a sub-sample of fast rotators from those identified as regular rotators in the Q-MANGA-GALEX sample. We matched to within ± 2.5 % of the stellar mass of the slow rotators to give 101 fast rotators, example velocity maps for which are shown in the bottom row of Figure 3. We shall refer to this sample of 202 galaxies as the MM-Q-MANGA-GALEX sample. An Anderson-Darling (AD) test reveals that the distribution of stellar masses of the fast rotators and slow rotators within this sample are statistically indistinguishable ($p = 0.25$). Similarly their redshift distributions are also statistically indistinguishable ($p = 0.10$).

We also consider the environmental densities of the fast and slow rotators by using estimates of the projected 5th nearest neighbour density, $\log \Sigma_5$, from Bamford et al. (2009). An Anderson-Darling (AD) test reveals that the distribution of environment densities of the 77 slow rotators and 88 fast rotators within the MM-Q-MANGA-GALEX sample with $\log \Sigma_5$ measurements are statistically indistinguishable ($p = 0.23$).

This is surprising since the current thinking is that slow rotators are more likely to be the central galaxy of a group or cluster, whereas fast rotators are more likely to be satellite galaxies (see extensive review by Cappellari 2016; **?**; **?**, and references therin).

Given the above statistical tests, the only difference between the regular and non-regular rotators of the MM-Q-MANGA-GALEX sample is their kinematics.

2.4 SFH Inference

STARPY[1] is a PYTHON code which allows the inference of the exponentially declining star formation history (SFH) of a single galaxy using Bayesian Markov Chain Monte Carlo techniques (Foreman-Mackey et al. 2013)[2]. The code uses the solar metallicity stellar population models of (Bruzual & Charlot 2003, hereafter BC03), assumes a Chabrier IMF

[1] Publicly available: `http://github.com/zooniverse/starpy`
[2] `http://dan.iel.fm/emcee/`

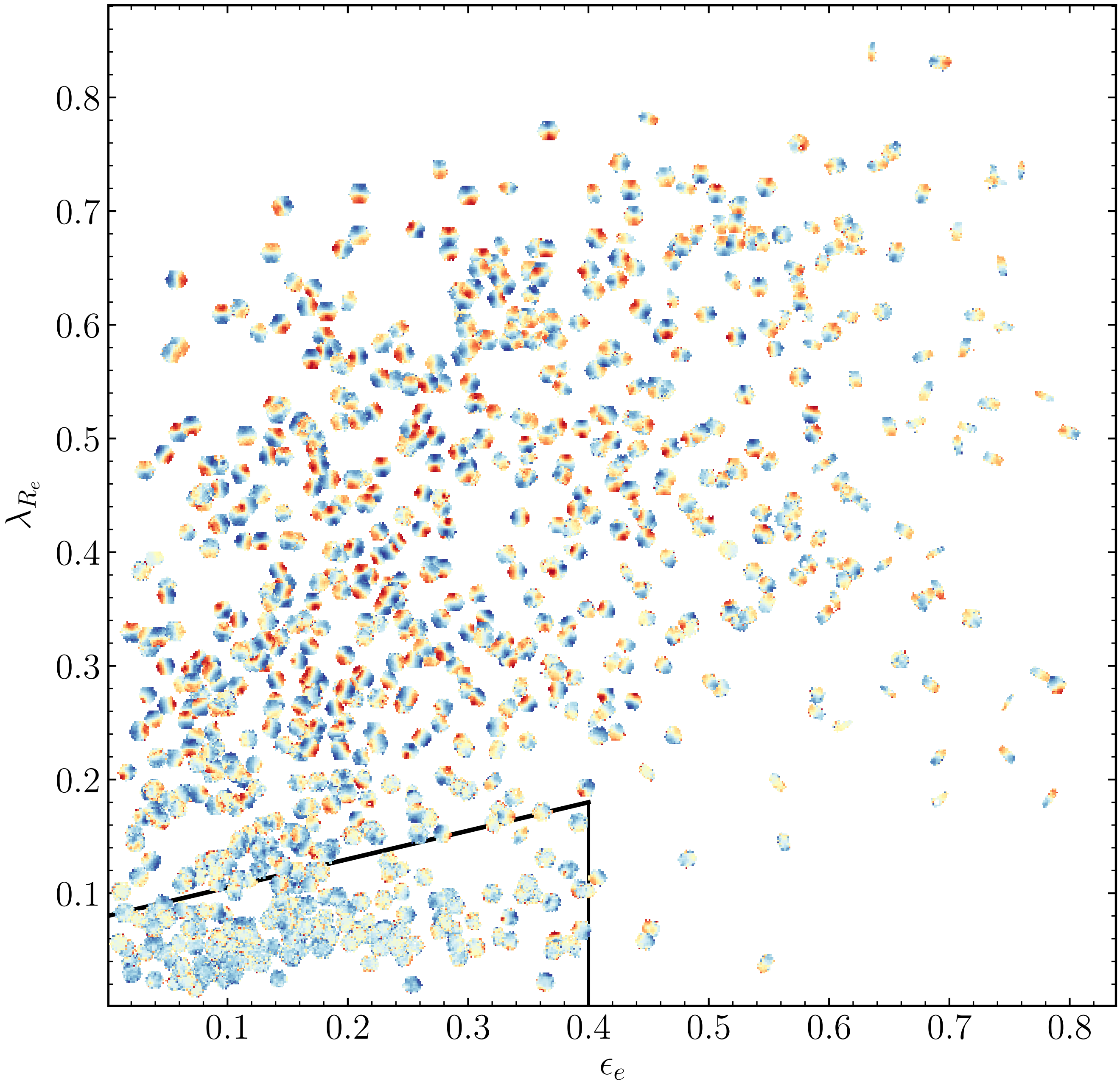

Figure 2. Ellipticity versus stellar angular momentum for the regular and non-regular rotators of the Q-MANGA-GALEX sample. Each point is shown by its stellar velocity map, each normalised to have a stellar velocity of 0 km s^{-1} shown by the colour yellow. We show the separation between regular (i.e. fast) and non-regular (i.e. slow) rotators from Cappellari (2016) with the solid black line.

(Chabrier 2003) and requires the input of the observed $u-r$ and $NUV-u$ colours and redshift. No attempt is made to model for intrinsic dust.

The SFH is described by an exponentially declining SFR described by two parameters; the time at the onset of quenching, t_q [Gyr], and the exponential rate at which quenching occurs, τ [Gyr]. Under the simplifying assumption that all galaxies formed at $t = 0$ Gyr with an initial burst of star formation, the SFH can be described as:

$$SFR = \begin{cases} i_{sfr}(t_q) & \text{if } t < t_q \\ i_{sfr}(t_q) \times exp\left(\frac{-(t-t_q)}{\tau}\right) & \text{if } t > t_q \end{cases} \tag{3}$$

where i_{sfr} is an initial constant star formation rate dependent on t_q (Schawinski et al. 2014; Smethurst et al. 2015). A smaller τ value corresponds to a rapid quench, whereas a larger τ value corresponds to a slower quench. Note that a galaxy undergoing a slow quench is not necessarily quiescent by the time of observation. Similarly, despite a rapid quenching rate, star formation in a galaxy may still be on-

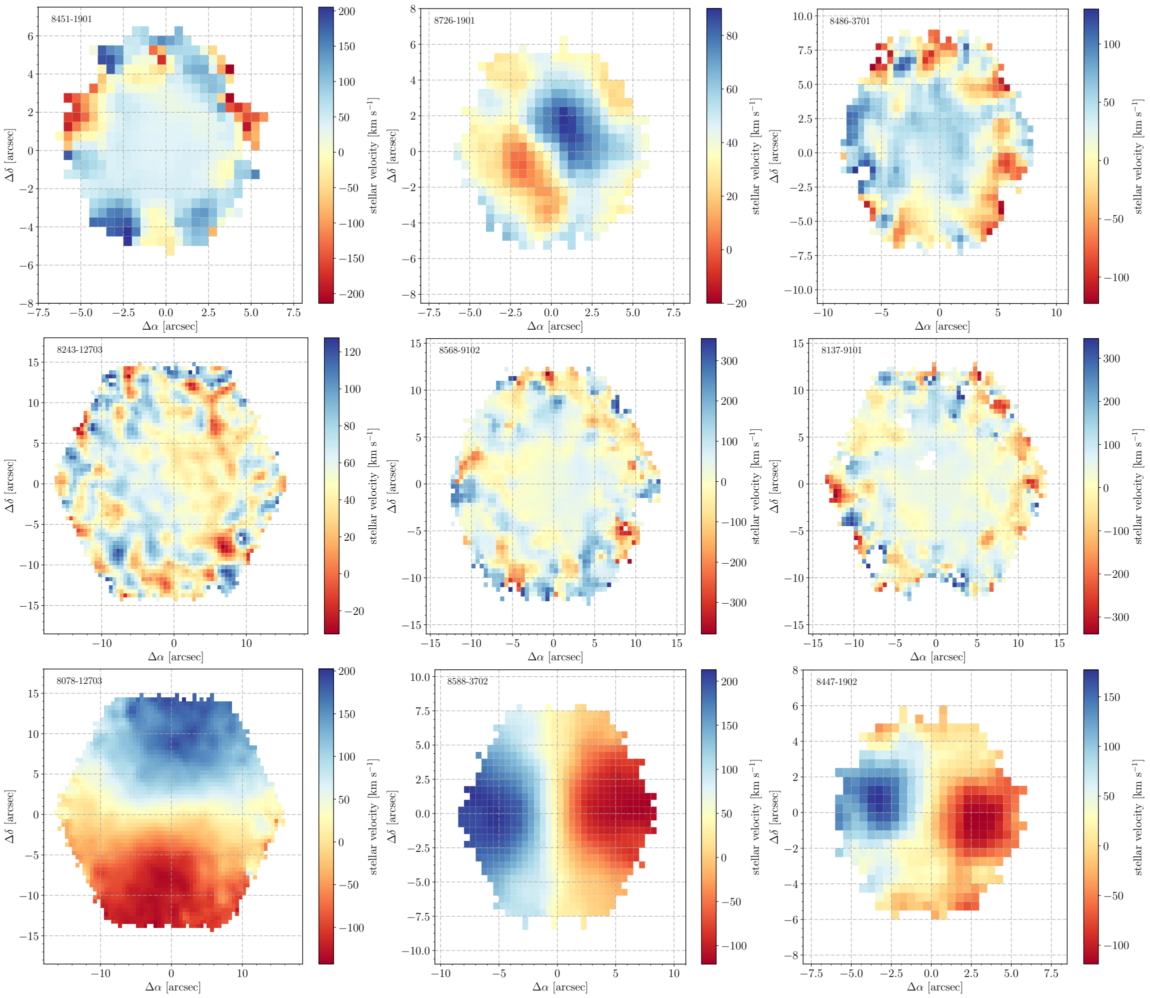

Figure 3. Example stellar velocity maps showing (top row) three galaxies removed from the non-regular rotator Q-MANGA-GALEX sample as their kinematics were not dispersion dominated, (middle row) three slow rotator galaxies with dispersion dominated kinematics, and (bottom row) three fast rotator galaxies with rotationally supported kinematics. The MaNGA ID of each galaxy is shown in the top left of each panel.

going at very low rates, rather than being fully quenched. This SFH model has previously been shown to appropriately characterise quenching galaxies (Weiner et al. 2006; Martin et al. 2007; Noeske et al. 2007; Schawinski et al. 2014).

We assume a flat prior on all the model parameters and model the difference between the observed and predicted $u - r$ and $NUV - u$ colours as independent realisations of a double Gaussian likelihood function (Equation 2 in Smethurst et al. 2015). We also make the simplifying assumption that the age of each galaxy, $t_{\rm age}$ corresponds to the age of the Universe at its observed redshift, $t_{\rm obs}$.

The probabilistic fitting methods to these star formation histories for an observed galaxy are described in full detail in Section 3.2 of Smethurst et al. (2015), wherein the STARPY code was used to characterise the morphologically dependence of the SFHs of $\sim 126,000$ galaxies. Similarly, in Smethurst et al. (2016), STARPY was used to show the prevalence of rapid, recent quenching within a population of AGN host galaxies and in Smethurst et al. (2017) to investigate the quenching histories of group galaxies. An example posterior probability distribution output by STARPY is shown for a single galaxy in Figure 5 of Smethurst et al. (2015), wherein the degeneracies of the SFH model between recent, rapid quenching and earlier, slower quenching can be seen.

To study the SFH across a sample of many galaxies, these individual posterior probability distributions are stacked in $[t_q, \tau]$ space to give a single distribution for the sample. This is no longer inference but merely a method to visualise the results for a population of galaxies (see appendix section C in Smethurst et al. 2016 for a discussion on alternative methods which may be used to determine the parent population SFH). These distributions will be referred to as the population SFH densities.

3 RESULTS

We determine the population SFH densities for both the regular and non-regular rotators of the MM-Q-MANGA-GALEX sample. This is shown in Figure 4 for both the time that quenching occurs (left panel) and exponential rate of quenching (right panel) for the regular (black solid line) and non-regular (red dashed line) rotators. Uncertainties on the population densities (shown by the shaded regions) are de-

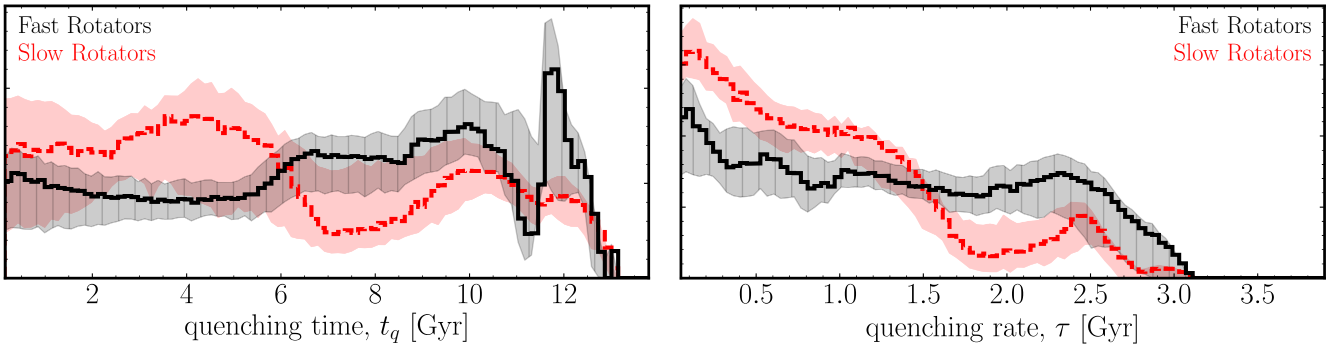

Figure 4. Population densities for the time, t_q (left) and exponential rate, τ (right) that quenching occurs in the MM-Q-MANGA-GALEX sample for the fast (black, solid) and slow (red, dashed) rotators. A high value of t_q corresponds to a recent quench, and a high value of τ corresponds to a slow quench. Shaded regions show the uncertainties on the distributions from bootstrapping.

termined from the maximum and minimum values spanned by $N = 1000$ bootstrap iterations, each sampling 90% of either the regular (black shaded region) or non-regular (red shaded region) rotators.

To statistically test the significance of our results, we estimate the 'best fit' $[t_q, \tau]$ values for each galaxy with the median value of an individual galaxy's posterior probability distribution from STARPY (i.e. the 50th percentile position of the MCMC chain). We test the distribution of these values of the regular and non-regular rotators in the MM-Q-MANGA-GALEX sample with AD-tests. Firstly, an AD-test on the distribution of t_q values for each galaxy, revealed that we cannot reject the null hypothesis that the regular and non-regular rotators quench at the same time ($AD \sim 0.3$, $p \sim 0.5$). Finally, an AD-test on the distribution of τ values for each galaxy, revealed that we can reject the null hypothesis that the fast and slow rotators quench at the same rate ($AD \sim 8.5$, $p \sim 0.0003$). This is a statistically significant (3.6σ) result, suggesting that non-regular rotators quench more rapidly than regular rotators of the same mass.

4 DISCUSSION

The results shown in Figure 4 suggest that regular and non-regular rotators are indeed separate populations quenched, and therefore formed, by different mechanisms. However, these quenching mechanisms appear to occur at similar cosmic times for regular and non-regular rotators. Our results contradict the results of the simulations of Khochfar et al. (2011) who find that the last major merger interaction for slow rotators was at $z \gtrsim 1.5$ (i.e. $t_q \lesssim 4.5$ Gyr). Contradicting the findings of Khochfar et al., Penoyre et al. (2017) find in the Illustris simulation that slow rotators only form after $z < 1$ (i.e. $t_q \gtrsim 6$ Gyr). We note that STARPY is not very sensitive to the time of quenching, particularly at early times i.e. $t_q \lesssim 6$ Gyr when $z \gtrsim 1$. Therefore, with STARPY in its current form we cannot currently conclude which scenario our results favour. Future work altering our inference code to take spatial spectral information provided by MaNGA may help us to address this issue.

We find that a fraction of the regular rotator sample quench at very slow rates ($\tau \geqslant 3$ Gyr; right panel of Figure 4). Since the Q-MANGA-GALEX sample has not been selected by visual morphology, there will be regular rotators which are disc dominated (i.e. with bulge-to-total mass ratios of less than 0.5 which would historically have been classified as a late-type galaxy). This likelihood for slower quenching rates is therefore likely to be caused by the effects of secular evolution through morphological quenching, slowly moving these disk galaxies off the SFS. Using the morphological classifications of Galaxy Zoo 2 (GZ2 Lintott et al. 2011; Willett et al. 2013) we find that $\sim 25\%$ of the regular rotators of the MM-Q-MANGA-GALEX sample have a disk or featured debiased vote fraction, $p_d \geqslant 0.8$ (i.e. 80% of classifiers marked the galaxy as having either a disk or features), and a debiased merger vote fraction, $p_{\rm merger} < 0.223$ (i.e. is not currently undergoing a merger). This is consistent (but not analogous) with the fact that $27\pm^1_9\%$ of the regular rotator quenching rate population density (black line in the right panel of Figure 4) is found at quenching rates $\tau > 2$ Gyr. Conversely only 4 non-regular rotators ($\sim 5\%$) were classified as having a disc or features. Of these 4 galaxies 2 have a debiased odd vote fraction, $p_{\rm odd} \geqslant 0.3$, suggesting they are undergoing either an interaction or merger. Upon visual inspection, the other 2 galaxies are large disks with spiral structures lying outside of the MaNGA fibre bundle at > 1.5 R$_e$ and therefore outside of the 1R$_e$ radius within which λ_{R_e} was calculated.

For the non-regular rotators there is very little preference for slow quenching rates with $\tau \geqslant 2$ Gyr in the right panel of Figure 4. If we compare this with the results from Smethurst et al. (2015), who found that 26.1% of the quenching rate population density for galaxies in the red sequence visually classified as 'smooth' in GZ2 was at slow quenching rates (see left panel of their Figure 8). However, a 'smooth' visual classification in GZ2 will include both regular and non-regular rotators. It is only in this study that we have been able to investigate the difference in the SFHs of those galaxies which are truly dispersion dominated from those which are visually early-type but which are still rotationally supported.

The prevalence of rapid rates ($\tau \lesssim 1$ Gyr) in the non-regular rotators of the Q-MANGA-GALEX sample supports the theory that these galaxies are formed by major mergers, which are thought to cause quenching at such rates (Springel et al. 2005; Bell et al. 2006; Lotz et al. 2008, 2011; Smethurst et al. 2015). However, we also find evidence for regular rotators quenching at these same rapid rates. Simulations have recently shown that although major mergers (2:1 or 1:1 mergers) can cause rapid quenching of a galaxy, they do not necessarily destroy the disk dominated nature of a galaxy (Pontzen et al. 2016; Sparre & Springel 2016) and can form a regular rotator Bois et al. (2011). This is thought to mainly occur in gas rich major mergers (Bois et al. 2011) and is likely the explanation for the preference for rapid rates in the regular rotator sample seen in Figure 4. Ongoing follow up observations using the Green Bank Telescope (GBT16A-095 and GBT17A-012) to obtain HI profiles of MaNGA galaxies will help to test whether the regular rotators are indeed more gas rich than non-regular rotators in this sample.

However Bois et al. (2011) also show that a gas rich major merger can produce a non-regular rotator. Upon inspection, Bois et al. found that these tend to be those with kinematically decoupled cores, rather than the typical 'slow' rotators with dispersion dominated kinematics. We have made no attempt in this study to remove galaxies with kinematically decoupled cores (or even counter rotating cores) from our non-regular rotator sample, but such a study could be the focus of future work.

These first results studying this issue suggest that although the kinematics of regular and non-regular rotators are different in nature, the mechanisms which quench, and therefore evolve, these galaxies are very similar. However, in order to completely destroy the disk of a galaxy, some property in the formation/quenching mechanism must exceed some threshold. Since simulations have shown that it is possible for a disc to be retained in a dry major 1:1 mass ratio merger, this quantity cannot be the merger mass ratio as previously thought (Binney & Tremaine 1987; Bois et al. 2010; Tonini et al. 2016). Instead, our results showing similar quenching rates occurring across both regular and non-regular rotator samples, combined with the findings of recent simulations by Bois et al. (2011); Pontzen et al. (2016); Sparre & Springel (2016), suggest that the total gas mass fraction within a pair of merging galaxies, is what will ultimately decide the kinematic fate of a galaxy.

ACKNOWLEDGEMENTS

RJS gratefully acknowledges research funding from the Ogden Trust.

Funding for the Sloan Digital Sky Survey IV has been provided by the Alfred P. Sloan Foundation, the U.S. Department of Energy Office of Science, and the Participating Institutions. SDSS acknowledges support and resources from the Center for High-Performance Computing at the University of Utah. The SDSS web site is `www.sdss.org`.

SDSS is managed by the Astrophysical Research Consortium for the Participating Institutions of the SDSS Collaboration including the Brazilian Participation Group, the Carnegie Institution for Science, Carnegie Mellon University, the Chilean Participation Group, the French Participation Group, Harvard-Smithsonian Center for Astrophysics, Instituto de Astrofísica de Canarias, The Johns Hopkins University, Kavli Institute for the Physics and Mathematics of the Universe (IPMU) / University of Tokyo, Lawrence Berkeley National Laboratory, Leibniz Institut fr Astrophysik Potsdam (AIP), Max-Planck-Institut für Astronomie (MPIA Heidelberg), Max-Planck-Institut fr Astrophysik (MPA Garching), Max-Planck-Institut für Extraterrestrische Physik (MPE), National Astronomical Observatories of China, New Mexico State University, New York University, University of Notre Dame, Observatório Nacional / MCTI, The Ohio State University, Pennsylvania State University, Shanghai Astronomical Observatory, United Kingdom Participation Group, Universidad Nacional Autónoma de México, University of Arizona, University of Colorado Boulder, University of Oxford, University of Portsmouth, University of Utah, University of Virginia, University of Washington, University of Wisconsin, Vanderbilt University and Yale University.

REFERENCES

Abazajian K. N. et al., 2009, ApJS, 182, 543
Bamford S. P. et al., 2009, MNRAS, 393, 1324
Bell E. F., Phleps S., Somerville R. S., Wolf C., Borch A., Meisenheimer K., 2006, ApJ, 652, 270
Binney J., Tremaine S., 1987, Galactic dynamics
Blanton M. R., Eisenstein D., Hogg D. W., Schlegel D. J., Brinkmann J., 2005, ApJ, 629, 143
Blanton M. R., Roweis S., 2007, AJ, 133, 734
Bois M. et al., 2010, MNRAS, 406, 2405
Bois M. et al., 2011, MNRAS, 416, 1654
Brinchmann J., Charlot S., White S. D. M., Tremonti C., Kauffmann G., Heckman T., Brinkmann J., 2004, MNRAS, 351, 1151
Bruzual G., Charlot S., 2003, MNRAS, 344, 1000
Bundy K. et al., 2015, ApJ, 798, 7
Cappellari M., 2016, ARA&A, 54, 597
Cappellari M. et al., 2007, MNRAS, 379, 418
Cappellari M. et al., 2013, MNRAS, 432, 1862
Cardelli J. A., Clayton G. C., Mathis J. S., 1989, ApJ, 345, 245
Chabrier G., 2003, PASP, 115, 763
Drory N. et al., 2015, AJ, 149, 77
Duc P.-A. et al., 2011, MNRAS, 417, 863
Emsellem E. et al., 2011, MNRAS, 414, 888
Emsellem E. et al., 2007, MNRAS, 379, 401
Fang J. J., Faber S. M., Koo D. C., Dekel A., 2013, ApJ, 776, 63
Foreman-Mackey D., Hogg D. W., Lang D., Goodman J., 2013, PASP, 125, 306
Gunn J. E. et al., 2006, AJ, 131, 2332
Hayward C. C., Torrey P., Springel V., Hernquist L., Vogelsberger M., 2014, MNRAS, 442, 1992
Hopkins P. F., Hernquist L., Cox T. J., Kereš D., 2008, ApJS, 175, 356
Jarosik N. et al., 2011, ApJS, 192, 14
Johnston E. J., Aragón-Salamanca A., Merrifield M. R., 2014, MNRAS, 441, 333
Kauffmann G. et al., 2003, MNRAS, 341, 33
Khochfar S. et al., 2011, MNRAS, 417, 845
Law D. R. et al., 2016, AJ, 152, 83
Law D. R. et al., 2015, AJ, 150, 19
Lintott C. et al., 2011, MNRAS, 410, 166
Lotz J. M., Jonsson P., Cox T. J., Croton D., Primack J. R., Somerville R. S., Stewart K., 2011, ApJ, 742, 103

Lotz J. M., Jonsson P., Cox T. J., Primack J. R., 2008, MNRAS, 391, 1137
Martin D. C. et al., 2005, ApJ, 619, L1
Martin D. C. et al., 2007, ApJS, 173, 342
Naab T. et al., 2014, MNRAS, 444, 3357
Noeske K. G. et al., 2007, ApJ, 660, L43
Oh K., Sarzi M., Schawinski K., Yi S. K., 2011, ApJS, 195, 13
Padmanabhan N. et al., 2008, ApJ, 674, 1217
Peng Y.-j. et al., 2010, ApJ, 721, 193
Penoyre Z., Moster B. P., Sijacki D., Genel S., 2017, ArXiv e-prints, 1703.00545
Pontzen A., Tremmel M., Roth N., Peiris H. V., Saintonge A., Volonteri M., Quinn T., Governato F., 2016, ArXiv e-prints, 1607.02507
Schawinski K. et al., 2014, MNRAS, 440, 889
SDSS Collaboration et al., 2016, ArXiv e-prints, 1608.02013
Smee S. A. et al., 2013, AJ, 146, 32
Smethurst R. J., Lintott C. J., Bamford S. P., Hart R. E., Kruk S. J., Masters K. L., Nichol R. C., Simmons B. D., 2017, ArXiv e-prints, 1704.06269
Smethurst R. J. et al., 2016, MNRAS, 463, 2986
Smethurst R. J. et al., 2015, MNRAS, 450, 435
Snyder G. F., Cox T. J., Hayward C. C., Hernquist L., Jonsson P., 2011, ApJ, 741, 77
Sparre M., Springel V., 2016, ArXiv e-prints, 1610.03850
Springel V., Di Matteo T., Hernquist L., 2005, ApJ, 620, L79
Stott J. P. et al., 2016, MNRAS, 457, 1888
Stoughton C. et al., 2002, AJ, 123, 485
Tonini C., Mutch S. J., Croton D. J., Wyithe J. S. B., 2016, MNRAS, 459, 4109
Toomre A., Toomre J., 1972, ApJ, 178, 623
Veale M. et al., 2017, MNRAS, 464, 356
Wake D. A. et al., 2017, ArXiv e-prints, 1707.02989
Weiner B. J. et al., 2006, ApJ, 653, 1049
Willett K. W. et al., 2013, MNRAS, 435, 2835
Yan R. et al., 2016, AJ, 152, 197
York D. G. et al., 2000, AJ, 120, 1579